



FCTUC FACULDADE DE CIÊNCIAS
E TECNOLOGIA
UNIVERSIDADE DE COIMBRA

DEPARTMENT OF MECHANICAL
ENGINEERING

A Compact Twisted String Actuation System for Robotic Applications

Dissertation presented to achieve the degree of Master in Mechanical Engineering in the specialization of Production and Project

Author

Rafael José Correia Batista

Supervisors

Prof. Dr. Mahmoud Tavakoli

Prof. Dr. Pedro Neto

Jury

President Professor Doctor **Cristóvão Silva**
Professor from University of Coimbra

Professor Doctor **Fernando Antunes**
Professor from University of Coimbra

Professor Doctor **Mahmoud Tavakoli**
Post-doc researcher from Institute of Systems and Robotics

Institutional Collaboration



Institute of Systems and Robotics of the University of Coimbra

Coimbra, September, 2014

Acknowledgements

This research work wouldn't be possible without the help of quite a few people. Thus I would like to thank to:

Professor Doctor Mahmoud Tavakoli for the support, advice and guidance provided, and for the opportunity to work in his research team.

Professor Doctor Pedro Neto for all the help and support and for allowing me to join this project.

All my colleagues at the lab for making these months such a fun and rewarding experience.

All the teachers and professors that helped me reach this stage.

My family and friends for everything.

Thank you.

Abstract

The research presented here, focus on the development of a compact twisted string actuation system for robotic applications. When coupled to a motor, a twisted string system acts as a high ratio rotary to linear motion convertor.

This dissertation starts with a brief description of existing applications of twisted string mechanisms. Then, the first prototype of the twisted string actuation system, built for this research, is presented. The prototype was used for the development of a better understanding of the mechanism and to find its capabilities. Afterwards, and based on experiments performed with the first prototype, a two-phase twisted string actuation system that benefits from an overtwist phase is proposed. In this way, a higher contraction ratio compared to the state of the art could be achieved. Furthermore, since none of the previous mathematical models could predict the linear displacement of the system, for the overtwist phase, an improved mathematical model was developed that can accurately predict the linear displacement over the entire range of motion. Afterwards, the twisted string system was applied for the actuation of a robotic hand. The high contraction ratio that was achieved with the two-phase twisted string system, resulted in a compact and light rotary to linear motion conversion mechanism that could fit inside the palm of a robotic hand, which has around the same size of an adult human hand. Finally, there will be an overview of the most important achievements and conclusions of this research work, along with some future plans for further investigation.

Keywords Twisted string, Strand-muscle, Twist drive, Robotic hand, Linear actuator.

Content

Index of figures	ix
Index of tables	xi
List of abbreviations.....	xiii
List of symbols.....	xiii
Acronyms	xiii
1. INTRODUCTION.....	1
1.1. Main Motivation	2
1.1.1. Advantages of the twisted strings actuation system	2
1.1.2. Problems with current twisted strings actuation systems	2
1.2. Robotic Hand Project.....	3
1.3. Research Aspects	4
1.3.1. Testing of the system capabilities	4
1.3.2. Mathematical model	4
1.3.3. Backdrivability	5
2. STATE OF THE ART.....	7
2.1. Patents	10
2.1.1. Twisted Cord Actuator (United States Patent)	10
2.1.2. Motion Conversion Device (United States Patent)	10
3. EXPERIMENTATION PHASE	11
3.1. Experiment - Testing the lifting capabilities of the twisted string actuation system	11
3.1.1. Experimental Setup	11
3.1.2. Experimental Results.....	12
3.1.3. Backdrivability	13
3.2. Experiment – Relation between the rotation of the motor shaft and the linear displacement of the strings	14
3.2.1. Overtwist Phase	14
3.2.2. Experimental Setup	15
3.2.3. Experimental Results.....	16
3.3. Experiment – Comparison between different separators and motor shaft connectors	17

4.	MATHEMATICAL MODEL	19
4.1.	Mathematical model for systems with a separator	19
4.2.	String Bundle Diameter	20
4.3.	Variable vs. Constant Radius Model	22
5.	APPLICATION OF THE TWISTED STRING ACTUATION SYSTEM	27
5.1.	Design of the robotic hand.....	27
5.2.	Assembly of the robotic hand.....	30
5.3.	Control system for the robotic hand	34
6.	CONCLUSION.....	37
6.1.	Publications	38
7.	REFERENCES	39

INDEX OF FIGURES

Figure 1.1 – Basic concept of the twisting string actuation system. This image is from the paper by Palli et. al. [2].	1
Figure 1.2 – Example of a twisted string actuation system. This image is a Twist Drive mechanism and it is from the paper by Sonoda et. al. in [1].	1
Figure 1.3 – Robotic hand, where the tendons are pulled using a motor and pulley system.	3
Figure 1.4 – Fist prototype of the twisted string actuation system.	4
Figure 2.1 – Ballista siege engine at Caerphilly Castle, Wales. Where twisted rope is used as a torsion spring. The red rectangles highlight the torsion springs.	7
Figure 2.2 – The DEXMART Hand virtual prototype, from the paper by Palli et. al. in [2].	8
Figure 2.3 – Photo of the robotic hand from the paper by Godler et. al. in [10]. This hand uses 15 twisted strings actuation systems to control it.	8
Figure 2.4 – Prototype exoskeleton elbow from the paper by Popov et. al. in [6].	9
Figure 2.5 – Concept of dual-mode robot finger from the paper by Shin et. al. in [12].	9
Figure 2.6 – Drawings of the twisted cord actuator patent.	10
Figure 2.7 – Drawing of the motion conversion device patent.	10
Figure 3.1 – Twisted string actuation system. With an electric motor (blue), strings (green), connection between motor shaft and strings (yellow) and separator (red). Where L is the twisting zone length, α is the rotational angle of the motor shaft, x is the linear displacement of the strings and S is the distance between the holes of the separator.	11
Figure 3.2 – First experimental setup.	12
Figure 3.3 – Experimental results. Where the time it took for the system to lift different weights is compared for various twisting zone lengths.	13
Figure 3.4 – Snapshot of the twisted string system with 2 strings from 0 to 70 turns. As can be seen, overtwisting starts to happen after 20 turns. After 40 turns, overtwist is not evenly distributed over the twisting zone and local overtwist starts to happen, which can be seen in the 50 turns snapshot.	14
Figure 3.5 – Experimental results for various number of strings in the system. Where x is the linear displacement and α is number of turns at the output shaft of the gearmotor.	17
Figure 3.6 – Different separators (red) and motor shaft connectors (yellow) tested. The distance between the holes of the separator, S , remains the same in all of the parts.	18

Figure 3.7 – Comparison of the variation of the linear displacement, x , with the number of turns at the output shaft of the gearmotor, α , for the various separators and connectors tested. 18

Figure 4.1 – String schematics, where L is the length of the twisting zone, α is the rotation angle of the motor shaft, r is the radius of the string bundle, X is the length of the strings inside the twisting zone, S is the distance between the holes in the separator and β is helix angle. 20

Figure 4.2 – Difference in diameter between the existing (right) and the proposed (left) string sections models. The numbers represent the string pairs. 22

Figure 4.3 – Comparison between the mathematical models and the experimental results. Where x is the linear displacement and α is number of turns at the output shaft of the gearmotor. 24

Figure 4.4 – Zoom of strings under twisting close to the separator. The red rectangle highlights the zone where the strings twist when they come out of the separator. In that zone the string bundle diameter remains constant for the entire range of overtwisting. 25

Figure 5.1 – 3D model of the robotic hand. It is possible to see the internal structures of the fingers (black), the main structure of the hand (green) and the palm cover (orange). 28

Figure 5.2 – Another view of the 3D model of the hand, now the back cover of the hand (yellow) is visible. 28

Figure 5.3 – Image of the internal components of the hand. It is possible to see the motors (blue), the encoders and switches (light blue), the spur gear that drives the thumb (brown), the connector between the motor shaft and the strings (yellow), the separator (red), the connection between the strings that twist and the tendons of the fingers (purple) and the motors mounting bracket that also routes the strings (orange). 29

Figure 5.4 – Image of the internal components of the hand. It is possible to see the circuit board (light green) and the encoders and switches (light blue). 29

Figure 5.5 – Image of the internal components of the hand. 31

Figure 5.6 – Image of the hand with the palm cover placed. 31

Figure 5.7 – Image of the hand with three of the fingers connected to the twisted string actuation system. 32

Figure 5.8 – Zoom of the twisted string system after a few turns of the motor shaft. 32

Figure 5.9 – Photo of the robotic hand with all of the fingers placed. 33

Figure 5.10 – Comparison of the robotic hand with a human one. 34

Figure 5.11 – Photo of the circuit board located inside of the hand. 34

Figure 5.12 – Photo of both circuit boards used to control the hand. 35

Figure 5.13 – Image of the GUI used to control the motors. 35

INDEX OF TABLES

Table 1.1 – Comparison between the contraction ratios of various existing systems.	2
Table 3.1 – Start of overtwist for various number of strings.	15
Table 3.2 – Dimensions of the twisted string actuation system.	16
Table 4.1 – String bundle diameter.	21
Table 5.1 – Motors used in the robotic hand.	30

LIST OF ABBREVIATIONS

List of symbols

L – Twisting zone length

α – Rotational angle of the motor shaft

x – Linear displacement of the strings

S – Distance between the holes of the separator

r – Radius of the string bundle

X – Length of the strings inside the twisting zone

β – Helix angle

Acronyms

ISR - Institute of Systems and Robotics of the University of Coimbra

DEXMART – Dexterous and autonomous dual-arm/hand robotic manipulation with smart sensory-motor skills: A bridge from natural to artificial cognition

CAD – Computer-Aided Design

GUI – Graphical User Interface

1. INTRODUCTION

A twisted string actuation system is a linear actuator that can be used in many robotic applications. This type of actuator works by using a motor to twist one or more strings. When the strings are twisted they contract and apply a linear displacement and a linear force on the driven object (Figure 1.1 demonstrates this concept). So, the strings mimic the way our own muscles work. This makes a twisted string actuation system very useful for tendon driven mechanisms, such as robotic hands and exoskeletons. The Figure 1.2 shows an example of a twisted string actuation system proposed by Sonoda et. al. in [1].

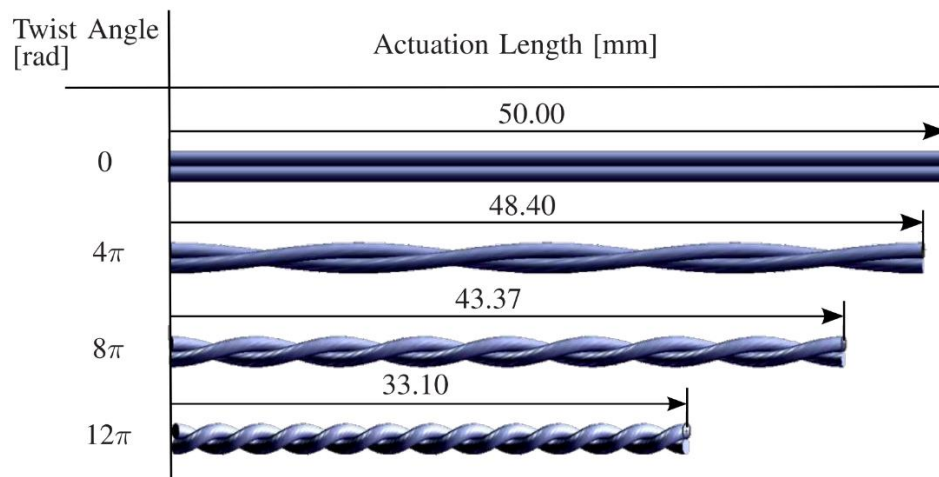


Figure 1.1 – Basic concept of the twisting string actuation system. This image is from the paper by Palli et. al. [2].

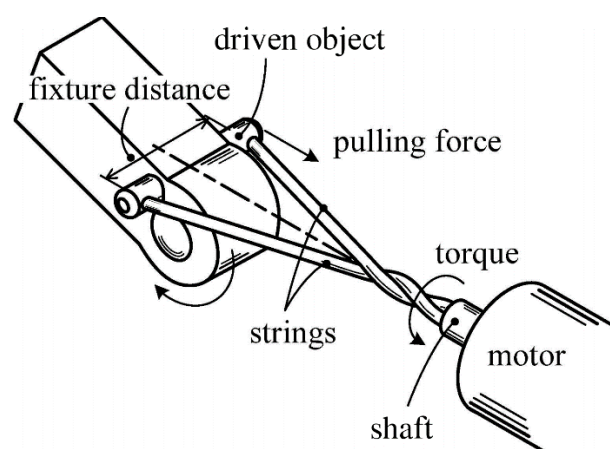


Figure 1.2 – Example of a twisted string actuation system. This image is a Twist Drive mechanism and it is from the paper by Sonoda et. al. in [1].

1.1. Main Motivation

The main motivation of this research is to develop a compact twisted string actuation system for robotic applications. This type of system is very useful for applications that require a linear actuator. By using the strings to transform the rotary motion of the motor into a linear motion, it is possible to use motors with a very high speed and low torque to move relative heavy loads.

1.1.1. Advantages of the twisted strings actuation system

Twisted string actuation systems offer several advantages over conventional systems, like a rack and pinion, or a lead screw and nut systems, such as being lighter, simpler and less expensive. The actuator is also not completely rigid, due to the strings elastic behavior. This can make it harder to control but it should be safer to operate around humans, due to the natural compliance of the entire system.

1.1.2. Problems with current twisted strings actuation systems

One of the major disadvantages of existing twisted string actuation systems is that they need to be larger than conventional systems. This is because the contraction ratio (the relation between the length of the system and the linear displacement it can achieve) of existing systems is around 25 %. Therefore, when an application requires a compact system, the twisted string actuation system is usually not an option. The Table 1.1 compares the contraction ratios of existing systems. The length of the system parameter refers to the size of the twisting strings, ignoring essential parts of the system like the actuators.

Table 1.1 – Comparison between the contraction ratios of various existing systems.

Previous works	Length of the system [mm]	Maximum linear displacement [mm]	Contraction [%]
[3]	55	13	24
[4]	200	28	14
[5]	235	28	12
[6]	250	60	24

Another problem of the twisted string actuation system is that the transmission ratio is not constant, like in conventional systems, such as geared systems. So designing a twisted string actuation system is harder because the non-linearity of the transmission ratio needs to be accounted for. However, the non-linearity of the transmission ratio, makes the system more adaptable to certain situations.

1.2. Robotic Hand Project

This research is integrated on the development of a robotic hand project (Figure 1.3). The study of the possible application of a twisted string actuation system to operate the robotic hand was the main contribution of this research to the hand project. Because of the above mentioned limitation of a small contraction ratio, the twisted string actuation system had to be placed in the forearm instead of inside the hand itself. In order to completely close the hand, the tendons inside the fingers need to be pulled around 35 mm. So, if current systems have a contraction percentage of around 25% the twisted string actuation system needs to have around 140 mm of length, which makes it impossible to fit inside a human sized hand. This limits the possible use of the hand as a prosthetics device. A study of the twisted strings mechanism was required, to find out if it was possible to make it more compact and thus more useful as a prosthetic device.

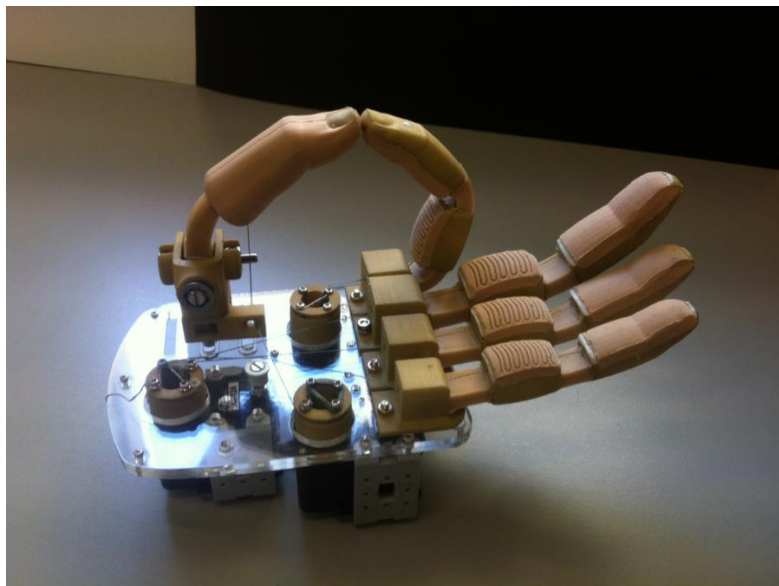


Figure 1.3 – Robotic hand, where the tendons are pulled using a motor and pulley system.

1.3. Research Aspects

1.3.1. Testing of the system capabilities

The first step in this research after the state of art was to build a first prototype of the twisted string actuation system (Figure 1.4), where the various parameters of the system could be easily changed. This first prototype was used to test the system capabilities and to develop a better understanding of the system itself.

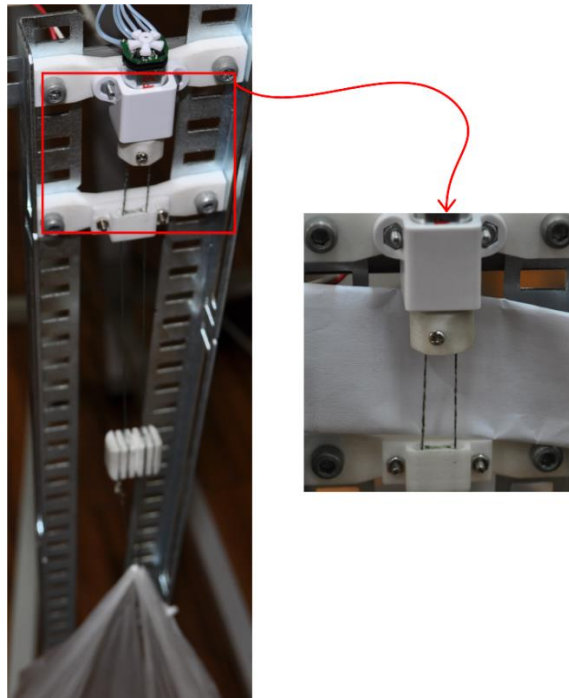


Figure 1.4 – First prototype of the twisted string actuation system.

1.3.2. Mathematical model

The development of a mathematical model that can predict the behavior of the twisted string actuation system was also a major step in this research. This is because existing mathematical models were only able to predict the systems behavior in a limited range of motion. Refinement of the existing mathematical models was essential for the understanding of the system behavior and made the development of an improved twisted string actuation system possible.

1.3.3. Backdrivability

Another important aspect to study was whether or not the system is backdrivable. To use the twisted string actuation system to operate the robotic hand, the system should be non-backdrivable. Because if the system is non-backdrivable, when the fingers need to hold a fixed position, the motors can be turned off. Otherwise battery will be wasted trying to hold a fixed position with the motors.

2. STATE OF THE ART

The twisted string systems have been used by humanity for millennia. The ancient Greeks used it for warfare in the form of torsion siege engines, where sinew rope was twisted to form a torsion spring. This simple but powerful device was used in warfare until the invention of gunpowder made it obsolete. Figure 2.1 shows an example of a torsion siege engine.

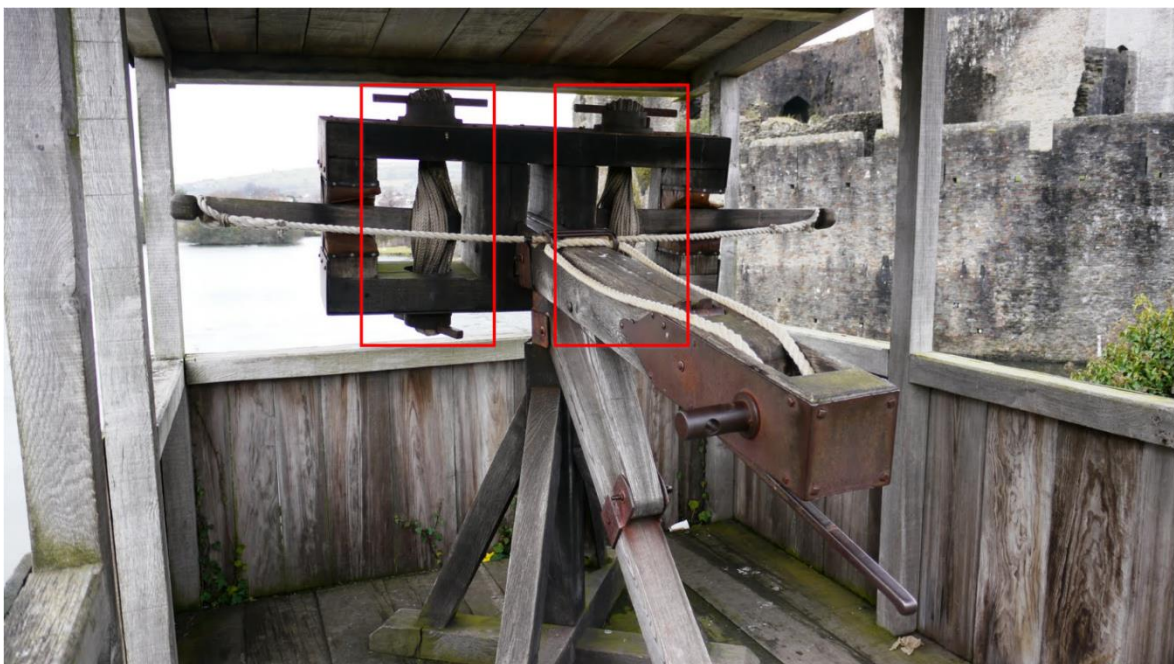


Figure 2.1 – Ballista siege engine at Caerphilly Castle, Wales. Where twisted rope is used as a torsion spring. The red rectangles highlight the torsion springs.

More recently, twisted string actuation systems have been used in robotics in the form of linear actuators, mostly in tendon driven mechanisms. Some of the earliest applications of the twisted string actuation systems in robotics was reported by M. Suzuki et. al., where they were used to drive a six-legged robot [7] and also an articulated arm that includes an anthropomorphic robotic hand [8, 9]. As reported in [9], actuators of the anthropomorphic hand are placed in the forearm of the system outside the hand itself. This is same for the DEXMART Hand [2], where several actuators with twisted string actuation systems are placed outside the palm and in a relatively large forearm. The Figure 2.2 shows a virtual prototype of the DEXMART Hand.

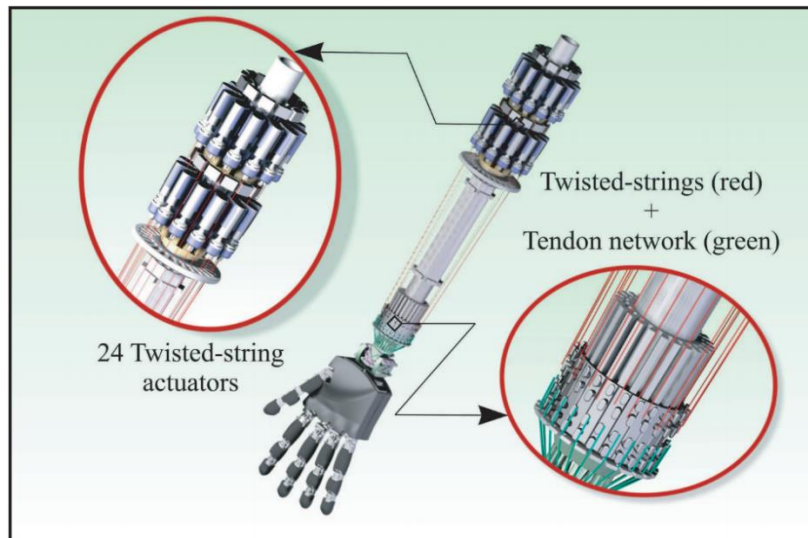


Figure 2.2 – The DEXMART Hand virtual prototype, from the paper by Palli et. al. in [2].

Godler et. al. presented a five fingered robotic hand in [10], that uses 15 twist drives to control the fingers (Figure 2.3). In this case the actuators are placed in the fingers. To do so and in order to increase the joints motion range with a limited stroke of the twisted string actuation system, the coupling point of the tendon was shifted from the joint at the cost of making the fingers larger. The use of so many actuators ultimately led to a relatively large and heavy hand. It weighs approximately 800 g, which makes it too heavy to be used as a prosthetic device.

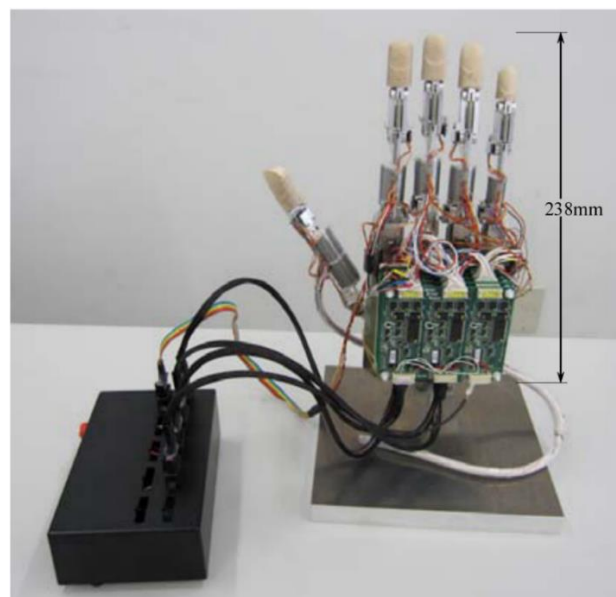


Figure 2.3 – Photo of the robotic hand from the paper by Godler et. al. in [10]. This hand uses 15 twisted strings actuation systems to control it.

An exoskeleton elbow controlled by a twisted string mechanism was proposed by Popov et. al. in [6, 11]. They also introduce the use of a separator to limit the twisting zone and by doing so they prevent the strings from twisting in undesirable areas. The Figure 2.4 shows the prototype exoskeleton elbow.

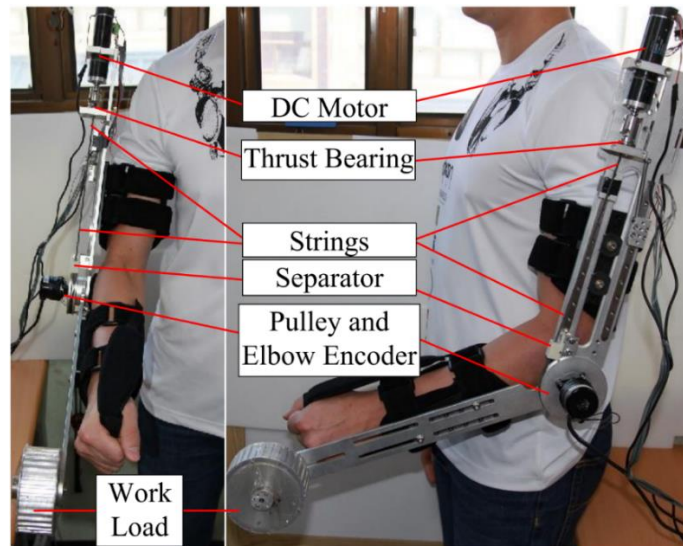


Figure 2.4 – Prototype exoskeleton elbow from the paper by Popov et. al. in [6].

Shin et. al. developed a dual-mode finger capable of two operating modes, a high speed motion and large grasping force [12]. By using a twisted string mechanism that uses a passive clutch to change both the length of the twisting zone and the radius of the system. This change in radius and length causes the motion to become slower but will radically increase the force applied by the fingertip.

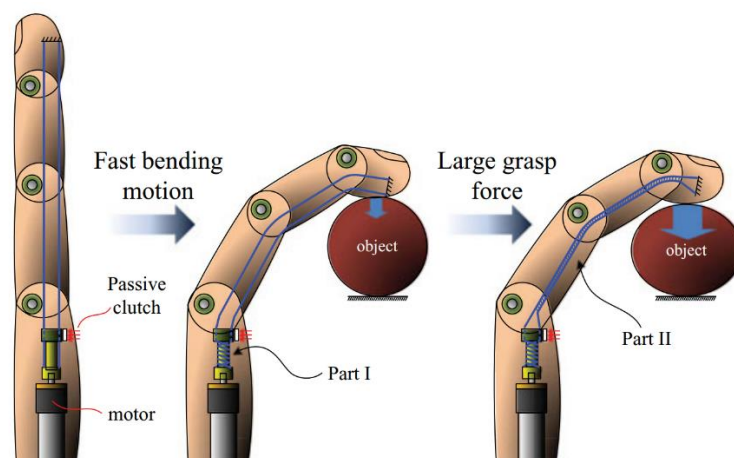


Figure 2.5 – Concept of dual-mode robot finger from the paper by Shin et. al. in [12].

2.1. Patents

2.1.1. Twisted Cord Actuator (United States Patent)

Inventor: Stephen R. Kremer

Filed: April 18, 1988

Patent Number: 4843921

The twisted cord actuator uses a motor to twist two or more strings, which will contract. This way the rotary motion of the motor is converted to linear motion.

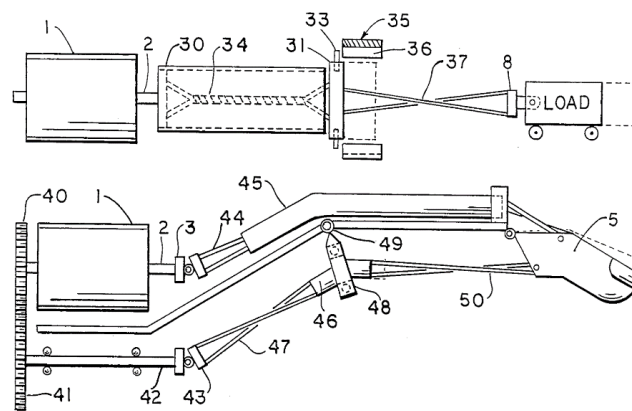


Figure 2.6 – Drawings of the twisted cord actuator patent.

2.1.2. Motion Conversion Device (United States Patent)

Inventor: Ivan Godler

Filed: March 4, 2009

Patent Number: US 8256310 B2

The motion conversion device also uses a motor to twist two strings and converts the rotary motion of the motor to a linear displacement of the driven object.

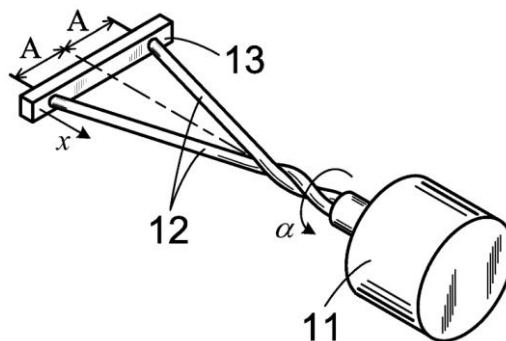


Figure 2.7 – Drawing of the motion conversion device patent.

3. EXPERIMENTATION PHASE

In order to better understand the capabilities of the twisted string actuation system a prototype was required. So after studying existing systems, the prototype was developed (Figure 3.2). It had the capability to change the various parameters of the system easily. This allowed for better study of the properties of the system and made comparisons with the predictions from the existing mathematical models possible.

To build the first prototype some parts were designed in a solid modeling CAD software and 3D printed in plastic. The Figure 3.1 shows the schematics of the system, the connection between motor shaft and strings (yellow) and the separator (red) parts were printed along with some other parts needed.

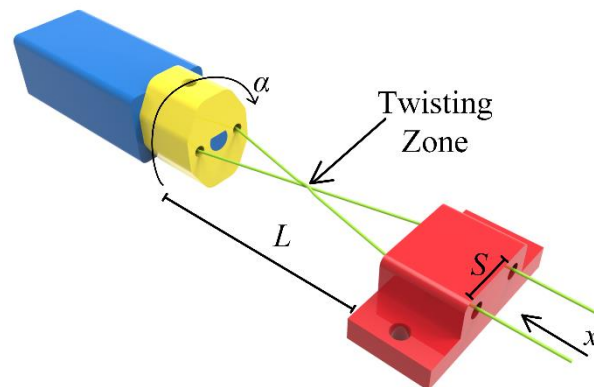


Figure 3.1 – Twisted string actuation system. With an electric motor (blue), strings (green), connection between motor shaft and strings (yellow) and separator (red). Where L is the twisting zone length, α is the rotational angle of the motor shaft, x is the linear displacement of the strings and S is the distance between the holes of the separator.

3.1. Experiment - Testing the lifting capabilities of the twisted string actuation system

3.1.1. Experimental Setup

The first experiment conducted with this prototype consisted in using the system to lift weights. The only system variable that was modified during the experiment was the length of the twisting zone, L . The motor used was a “10:1 Micro Metal Gearmotor HP” from Pololu, it has a nominal speed of 3000 r.p.m. and a stall torque of 0.028 Nm. The motor

was directly connected to a power supply with an output of 6 V and 1.6 A. The string used was the “Potenza Braided Line” from Vega, with a diameter of 0.35 mm. The strings are made of twisted strands of Dyneema which is a high-strength plastic.

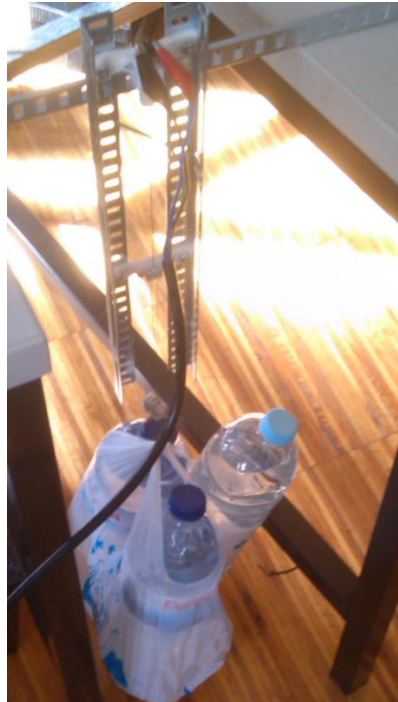


Figure 3.2 – First experimental setup.

The system was used to lift weights ranging from 2 kg to 4.5 kg. The weights started suspended (so the load was always constant) and were lifted 25 mm. The time it took to lift the weights for 25 mm was recorded.

3.1.2. Experimental Results

The results in Figure 3.3 show that increasing the length of the twisting zone increases the load the system can lift, however the system becomes slower. This is because the transmission ratio of the system changes with the length of the twisting zone.

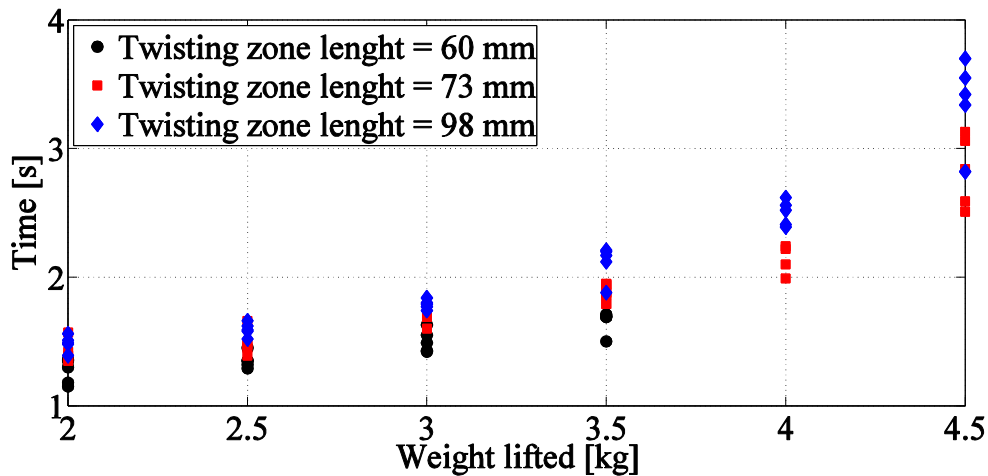


Figure 3.3 – Experimental results. Where the time it took for the system to lift different weights is compared for various twisting zone lengths.

Since the one of the main goals of this research is to make the twisted string actuation system more compact, what this results demonstrate is that by making the system more compact a motor capable of a higher torque output will be required.

3.1.3. Backdrivability

Another important observation of this first experiment was that the system was backdrivable. This is a problem, because if the system is backdrivable then the motors need to be powered on, in order to hold the fingers in a fixed position. Which will drain the battery faster and probably overheat the motors. However, the system will become non-backdrivable if a higher gear ratio motor like the “30:1 Micro Metal Gearmotor HP” and “100:1 Micro Metal Gearmotor HP” from Pololu are used. This is because the “Micro Metal Gearmotor HP” are essentially the same electrical motor coupled to different gearboxes. Since the electrical motor has an inherent inertia which is increased by the gearbox, then higher transmission ratio motors will have a higher inertia. From experience by using a motor like the “30:1 Micro Metal Gearmotor HP” or with an even higher transmission ratio, the system becomes non-backdrivable.

3.2. Experiment – Relation between the rotation of the motor shaft and the linear displacement of the strings

In this experiment, the objective was to understand the correlation between turns of the motor shaft and the linear displacement of the system. Before the description of the experiment itself it is important to explain the behavior of the strings under twisting.

3.2.1. Overtwist Phase

When the motor shaft rotates the strings start to twist evenly. However, after a few turns, when there isn't enough space for them to twist evenly, the strings start to twist around themselves. We call this phase the overtwist phase. In Figure 3.4 it is possible to see the overtwist phase happening after 20 turns. After 40 turns, overtwist is not evenly distributed over the twisting zone and local overtwists start to happen, which can be seen in 50 turns snapshot. After this stage, the string is not uniform anymore. Such local overtwists move along the strings in the twist zone as can be seen in 60 and 70 turns snapshots. These local overtwists will cause problems unwinding, because they will get stuck in the separator holes and need to be manually removed.

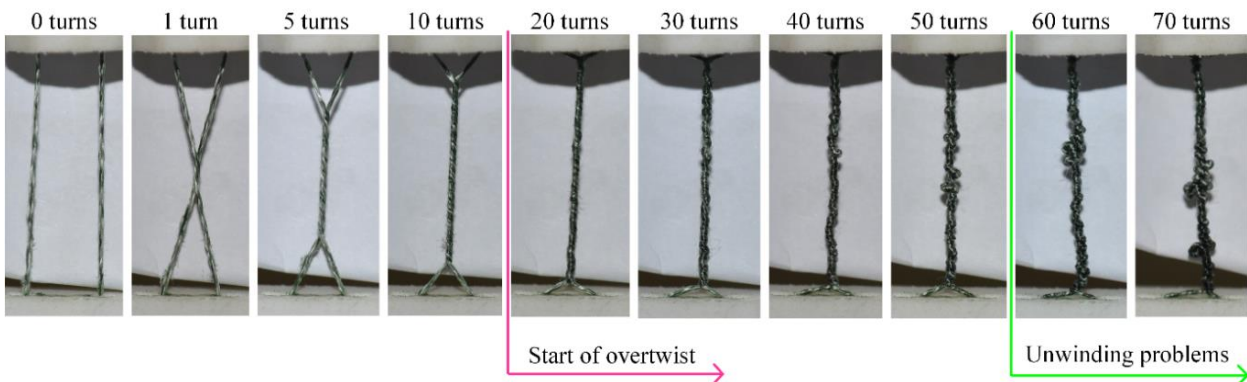


Figure 3.4 – Snapshot of the twisted string system with 2 strings from 0 to 70 turns. As can be seen, overtwisting starts to happen after 20 turns. After 40 turns, overtwist is not evenly distributed over the twisting zone and local overtwist starts to happen, which can be seen in the 50 turns snapshot.

Table 3.1 shows the amount of contraction and the number of turns where overtwist began for various number of strings. This is the result of observation during the experiments. The overtwist phase seems to start between 10% and 20% of contraction, which is about the maximum contraction percentage that similar twisted string systems have reported. The results presented in Table 3.1 demonstrate that the increase in diameter makes

the overtwist phase happen sooner (less turns). Since the length of the twisting zone is constant, then the volume of the strings inside the twisting zone increases with the additional strings. Because of this increase in volume, it is logical for the overtwist phase to happen sooner.

Table 3.1 – Start of overtwist for various number of strings.

Nr. of strings	Diameter of the string bundle [mm]	Contraction of the system [%]	Start of overtwist [turns]
2	0.47	19	20
4	0.63	9	11
6	0.86	10	10
8	0.94	10	8

The other research teams that studied this type of system either do not mention why they do not achieved higher contractions or say that the strings get damaged when they are twisted too much. In [13] the authors say *“In practice, the repetitive twisting of a string for a certain large angle will result in the rupture of the string after a number of cycles”*. However the "Potenza Braided Line" used in the experiments never suffered damage from overtwisting, even after hundred cycles of overtwisting. However, no experiment was performed specifically to test the life of the strings under overtwisting.

So, in order to reduce the size of the system, the overtwist phase will be used. This will allow for higher contraction ratios and possibly to fit the system inside the palm of a human sized robotic hand.

3.2.2. Experimental Setup

We used the “100:1 Micro Metal Gearmotor HP” from Pololu with 320 r.p.m. and 0.22 Nm of stall torque. The string which was used for this experiment, was the "Potenza Braided Line" from Vega with a diameter of 0.35 mm, which according to the manufacturer is capable of enduring loads up to 321 N and has a high resistance to wearing. We tested the twisted string actuation system, by lifting 2 kg weights with 2, 4, 6 and 8 strings and the

linear displacement for each turn of the motor was recorded. The dimensions of the system are shown in the Table 3.2.

Table 3.2 – Dimensions of the twisted string actuation system.

Nr. of Strings	Twisting zone length [mm]	Distance between the separator holes [mm]	Diameter of the string bundle [mm]
2	23.20	5	0.47
4	23.42	5	0.63
6	22.85	5	0.86
8	23.30	5	0.94

3.2.3. Experimental Results

Figure 3.5 shows the experimental results where the linear displacement is compared with the number of turns of the output shaft. By increasing number of strings, the diameter of the string bundle also increases. As can be seen in the image, at the same rotation input, higher displacements are possible with higher number of strings, due to the increase in diameter. The results which are present in Figure 3.5 show only the number of turns up to the point where the system starts to have problems untwisting. This problems occur because of the knots that form after several rounds of overtwisting (please check Figure 3.4 after 60 turns). In Figure 3.5 it is possible to observe that by increasing number of strings, untwisting problems happened at an earlier stage (less number of turns). Also, it is important to note that in this specific case, the 6 strings system is the one that was able to achieve the most linear displacement, x , and necessarily the biggest contraction percentage (81%). If the maximum contraction percentage of 81% is compared to existing systems, who only achieve a contraction of around 25% (please check Table 1.1), then it becomes clear that using the overtwist phase can potentially increase compactness.

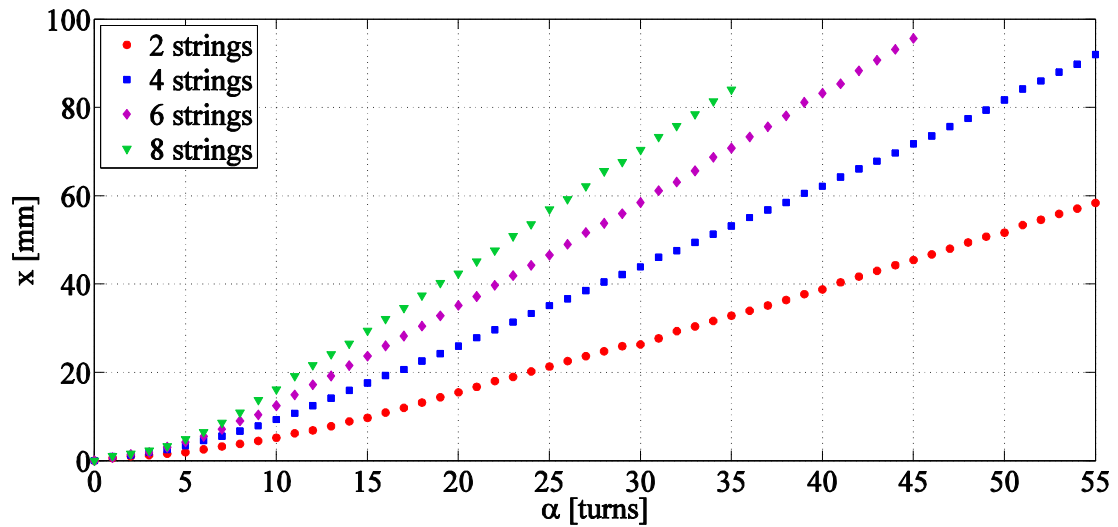


Figure 3.5 – Experimental results for various number of strings in the system. Where x is the linear displacement and α is number of turns at the output shaft of the gearmotor.

3.3. Experiment – Comparison between different separators and motor shaft connectors

The separator is used to limit the twisting of the strings to a certain area, the twisting zone. In this way, beyond the separator there is only linear motion of the strings and problems caused by the strings twisting in complicated areas are avoided.

In order to be able to increase the diameter of the string bundle, more strings need to be added. The strings can simply be passed through the two holes system, or more holes need to be added to accommodate all of the strings. To find if there is any difference in behavior due to the addition of the holes, both solutions were tested (please check Figure 3.6).

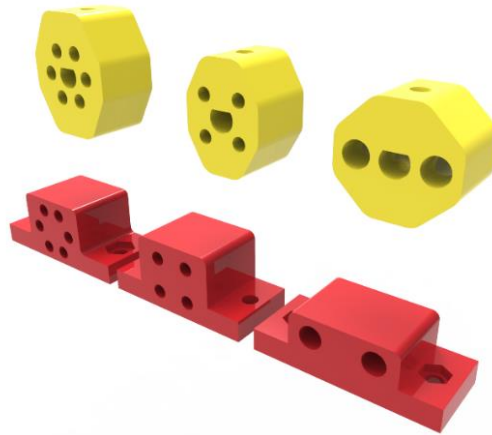


Figure 3.6 – Different separators (red) and motor shaft connectors (yellow) tested. The distance between the holes of the separator, S , remains the same in all of the parts.

Figure 3.7 shows the variation of linear displacements with the rotation of the motor shaft. Results show that the number of holes has no influence on the displacement of the system. However the systems with 4 and 6 holes had much less untwisting problems than the 2 holes system.

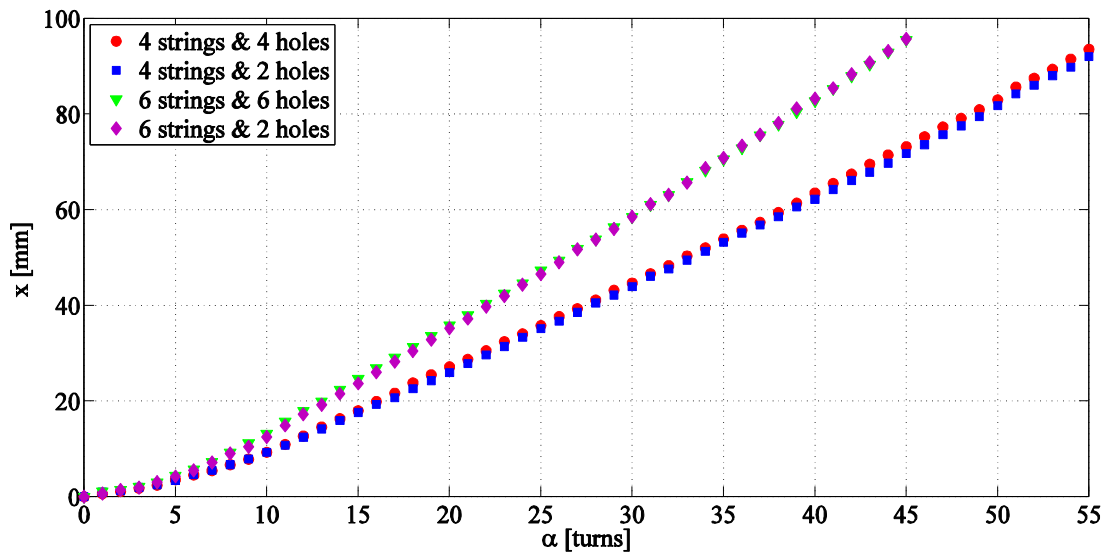


Figure 3.7 – Comparison of the variation of the linear displacement, x , with the number of turns at the output shaft of the gearmotor, α , for the various separators and connectors tested.

4. MATHEMATICAL MODEL

In order to be able to control the tendon based mechanisms with a twisted string actuation system, it is required to estimate the contraction of the strings, based on the position of the rotary actuator's shaft. None of the previously developed models could correctly fit our experimental results after around 15% of the contraction. After studying the previous models and our experiments, we performed some corrections to the models. First we added a new element, the distance between the holes in the separator (S). Second we developed an improved theory for prediction of the radius of the multi string system after they twist around each other. Finally we concluded that a constant radius model performs significantly better over the variable radius model for the long stroke range. The mathematical model presented here clearly outperforms previous models over a larger range of contraction.

The influence of the force applied was not considered in the prediction of the linear displacement. In the article [5], the authors stated that *"the change in the load force has insufficient influence on current mathematical model of the single twisted string transmission system"*. We only chose a 20 N load to test our system in the experiment in section 3.2, to be able to compare our results with similar works like [13] that used loads up to 31.5 N.

4.1. Mathematical model for systems with a separator

While the architecture of our system is similar to the system presented in [6, 11], we observed that the mathematical model presented in the articles can only predict the contraction up to 15% of the original length. One of the parameters that was not considered in [6] is S , the distance between the holes in the separator.

Figure 4.1 shows the schematic of the system that includes the S parameter. where L is the length of the twisting zone, α is the rotation angle of the motor shaft, r is the radius of the string bundle, X is the length of the strings inside the twisting zone, S is the distance between the holes in the separator and β is helix angle.

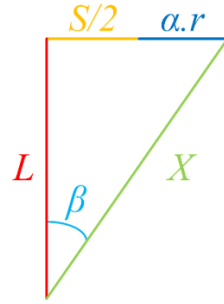


Figure 4.1 – String schematics, where L is the length of the twisting zone, α is the rotation angle of the motor shaft, r is the radius of the string bundle, X is the length of the strings inside the twisting zone, S is the distance between the holes in the separator and β is helix angle.

When the motor shaft rotates, only X , α and β will increase while the parameters L , r and S remain constant. If the length of the string inside the twisting zone, X , increases with the rotation of the motor shaft, then the linear displacement, x , is equal to the amount of string that enters the twisting zone. So the following equations can be used to calculate the linear displacement:

$$x = X - L, \quad (4.1)$$

$$x = \sqrt{L^2 + \left(\frac{S}{2} + \alpha \cdot r\right)^2} - L. \quad (4.2)$$

It should be noted that when the actuator rotates, the amount of α increases, and in this case S loses its significance over time. However it is quite an important parameter in the beginning, and also it adds an incremental error in each turn.

4.2. String Bundle Diameter

The second parameter that we studied in the above equation was the radius. Introducing the precise value of r to the mathematical model is very important. The significance of r in the equation increases by each rotation, since r is multiplied by the increasing α . While the radius of a single string in the twisting string system is constant, after twisting around each other, the radius of the entire string bundle is not a simple multiplication of the string radius and the number of strings. Palli et. al. suggested a model for estimating of the radius of the string bundle after twisting [4]. In their model it was

considered that always one of the strings forms a core, while the rest of the strings wrap around it.

In order to find the actual diameter of the strings, when they are twisted and loaded, we twisted the strings for 5 turns with a 2 kg load applied. Then we measured the diameter of the string bundle with a digital caliper. The results are present in Table 4.1.

Table 4.1 – String bundle diameter.

Nr. of strings	Measured Diameter [mm]	Model Diameter [mm]
1	0.24	0.24
2	0.47	0.48
4	0.63	0.66
6	0.86	0.87
8	0.94	0.87

However, the experimental measurements in Table 4.1 do not match the concept presented in [4]. Therefore a different model is proposed here, where the center core is made of two strings, rather than a single string, while any additional pair of strings wraps around the core, meaning that the other string pairs also wrap around the core at an equal distance from the core. This is a more valid assumption, because in a twisted string system, one string should wrap around another string, so the first two strings that meet each other form the core. Other strings also find their pair milliseconds after the first core is formed, so they should wrap around the first formed core. Figure 4.2 compares the two models and the predicted diameter of the string bundle from the model, on the left of the image, shows a much better correlation with the experimental results in Table 4.1. In Figure 4.2, number 1 to 4 show the pairs of the strings as they form the bundle. To describe how this format of strings is formed, we should consider the time that each pair of string reaches the core pair. For instance considering the 4 string case, when the second pair approaches the core, strings try to place themselves around the core and as near as possible to the center. Now to consider the case of 6 strings, we should first consider a four string bundle is already formed and the fifth and sixth string place themselves in a way to be as close as possible to the center (since the

twisting force slides them to the center). As can be seen, the new model is clearly more accurate than the previous model. It is also important to consider why the strings organize themselves in pairs. We believe the reason for this is that the axial load is unevenly distributed along the string pairs. The two string system, in reality, has only one string, since the two ends of the string are tied to the plastic part that connects the system to the weights. So the load is equal on the pair of strings of the two string system. When more strings are added, they are connected in the same way and because of this, each string in the pairs is equally loaded. However, different pairs may have different loads, because they are manually assembled and the length of each pair can be slightly different. Therefore strings wrap around the center at different times. For example, the pair with the higher axial load, is more stretched and reaches the center sooner and thus it forms the core.

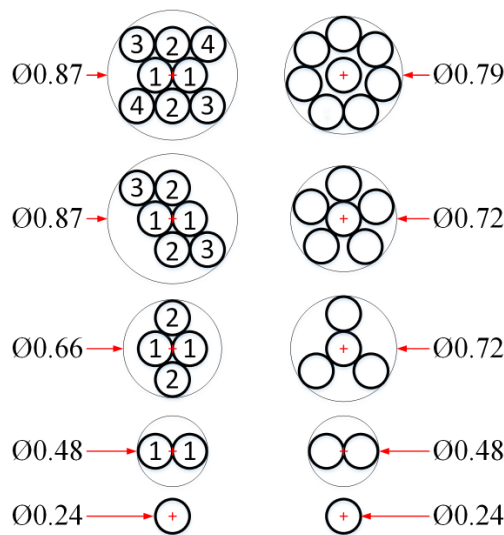


Figure 4.2 – Difference in diameter between the existing (right) and the proposed (left) string sections models. The numbers represent the string pairs.

4.3. Variable vs. Constant Radius Model

Another part of the mathematical model that we studied was the variable radius model. The model for twisted string actuation systems which is proposed in [5, 6, 11] presents a variable radius model to improve the correlation between the experimental results and the theory. The variable radius model considers that the radius of the string bundle will increase with twisting, because the length of the twisting zone is constant and the volume of string that enters the twisting zone keeps increasing. So it is logical that with twisting, the

radius of the string bundle increases accordingly. In the variable radius model, the radius varies according to the following equation:

$$r_{var} = r_0 \sqrt{\frac{L+x}{L}}, \quad (4.3)$$

where r_0 is the initial radius of the string bundle.

Figure 4.3 shows the comparison between the experimental results and variable radius model. As can be seen, the variable radius model fails to predict the displacement in the overtwisting phase and can only match the experimental result in the first phase. The reason for this, is that in the first phase the increase in the radius is uniformly distributed along the bundle in the twisting zone and when more string enters to the zone, the value of r parameter in Figure 4.1 and thus in equation (4.2) increases. But as can be observed in Figure 3.4, on the second phase, overtwisting happens locally in different zones of the string. This means that several knots are formed in different places until the bundle is filled with those knots. Thus when overtwisting happens, the radius of the string bundle stops to increase uniformly along the length of the twisting zone and the variable radius model is no longer valid.

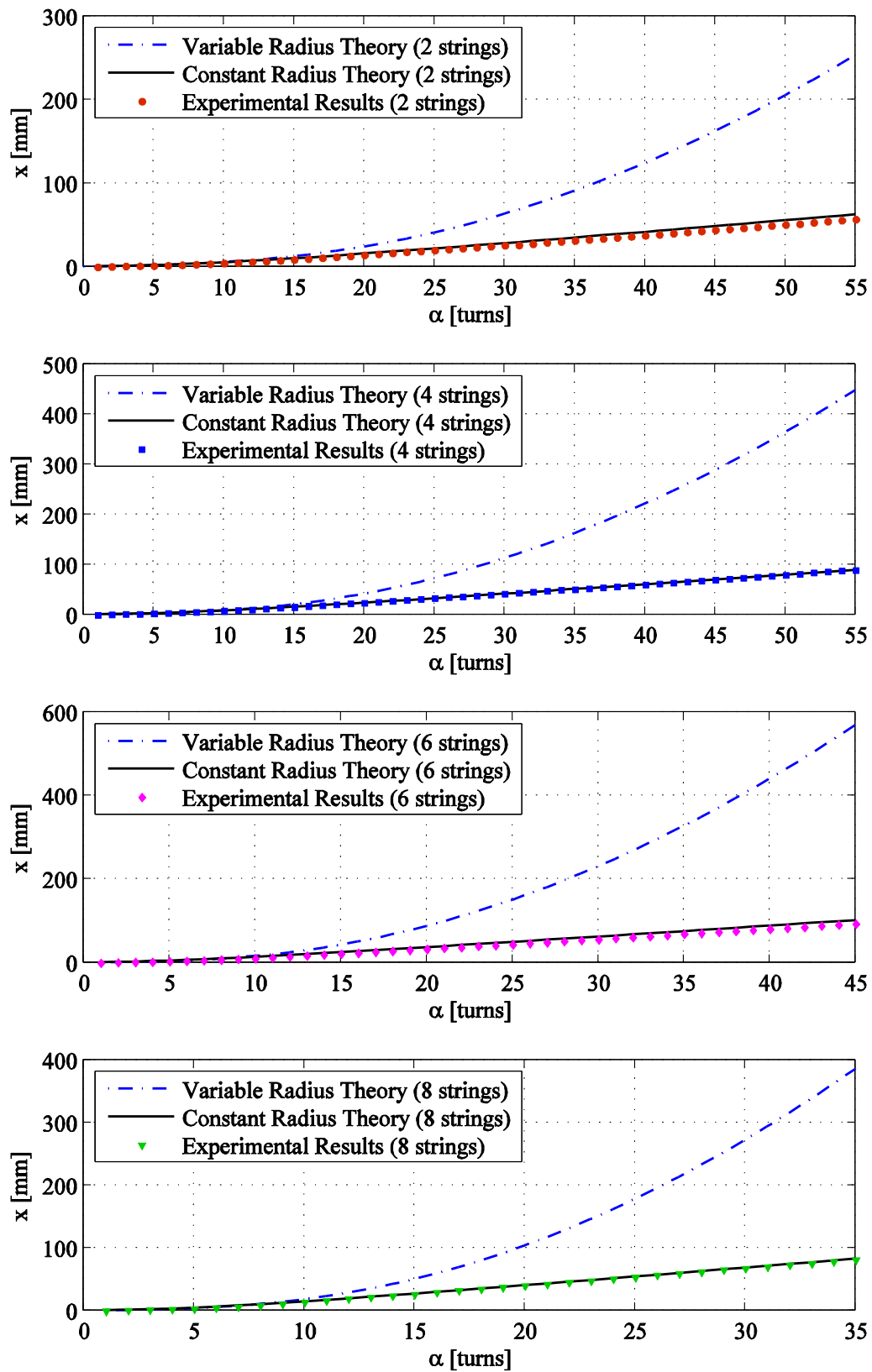


Figure 4.3 – Comparison between the mathematical models and the experimental results. Where x is the linear displacement and α is number of turns at the output shaft of the gearmotor.

Moreover, in Figure 4.4 it is possible to see that, in the area where the strings twist when they come out of the separator, the helix angle, β , and the radius, r , remain constant through the entire overtwisting phase. Since this is the place where the two strings actually twist around each other and the radius is constant in this part of the twisting zone, then this may be the reason for the constant radius model to work over the entire range of contraction, even if the radius increases in the rest of the twisting zone.



Figure 4.4 – Zoom of strings under twisting close to the separator. The red rectangle highlights the zone where the strings twist when they come out of the separator. In that zone the string bundle diameter remains constant for the entire range of overtwisting.

Figure 4.3 also compares the mathematical model presented in this section with the experimental results. This mathematical model takes into the account the distance between the holes in the separator (S), the corrected bundle diameter model and the constant radius theory. The model matches very well the experimental results in all cases of 2, 4, 6 and 8 strings.

5. APPLICATION OF THE TWISTED STRING ACTUATION SYSTEM

As was mentioned in section 1.2, this research work is a part of a bigger project that intends to develop a robotic hand for prosthetic and industrial manipulation applications. One of the main motivations behind this work was to integrate a twisted string actuation system in the hand and evaluate its practicality.

Therefore, in order to demonstrate the practicality of the twisted string actuation system and the compactness achieved by this research, a new version of the robotic hand was designed and built. In this version, twisted string actuation systems are used for flexion of all fingers. One twisted string actuation system is used for flexion of the thumb and the index finger and another similar system is used to close the remaining three fingers of the hand together. A third actuator is used for the thumb circumduction movement.

Because the fingers require a linear motion to close (the tendons are pulled), it is advantageous to use the twisted string actuation system as a linear actuator. However, in the case of the rotation of the thumb, if a twisted string actuation system is used, the rotary motion is converted to linear motion by the twisted string actuation system and then the linear motion needs to be converted back to a rotation by a pulley. With all of this conversions there is a loss of energy, which makes the use of a geared system advantageous.

5.1. Design of the robotic hand

The hand was designed in a solid modeling CAD software (please check from Figure 5.1 to Figure 5.4) and printed in plastic using a 3D printing service. The fingers (in black) were already previously designed, and their development is not part of this research. All of the following pictures are colored so that it is possible to distinguish the different parts.



Figure 5.1 – 3D model of the robotic hand. It is possible to see the internal structures of the fingers (black), the main structure of the hand (green) and the palm cover (orange).

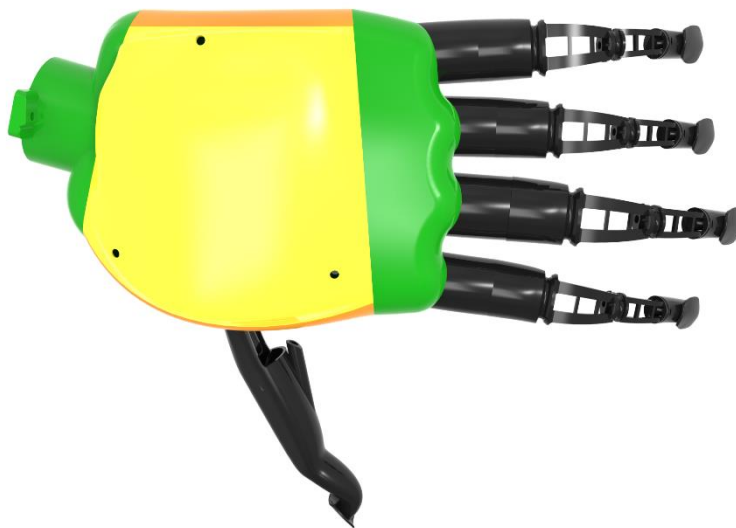


Figure 5.2 – Another view of the 3D model of the hand, now the back cover of the hand (yellow) is visible.

Figure 5.3 and Figure 5.4 show the hand with the palm cover and the back cover removed and it is possible to see the internal components.

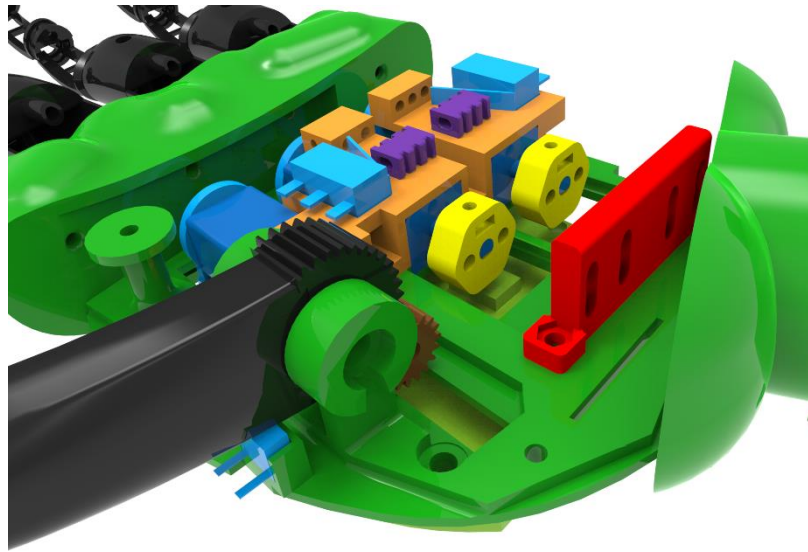


Figure 5.3 – Image of the internal components of the hand. It is possible to see the motors (blue), the encoders and switches (light blue), the spur gear that drives the thumb (brown), the connector between the motor shaft and the strings (yellow), the separator (red), the connection between the strings that twist and the tendons of the fingers (purple) and the motors mounting bracket that also routes the strings (orange).

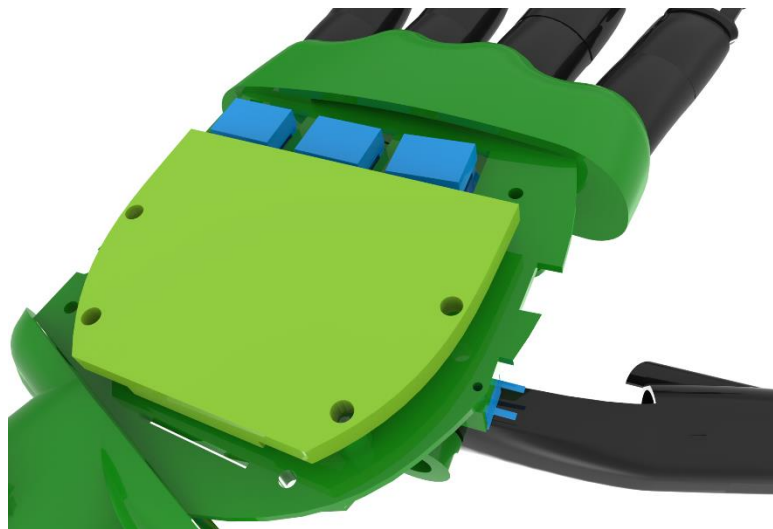


Figure 5.4 – Image of the internal components of the hand. It is possible to see the circuit board (light green) and the encoders and switches (light blue).

To control the hand there will be three actuators. Two motors will control the flexion of the fingers, while another motor will control the thumb circumduction. Based on the requirements of the project, to be able to completely close the hand the twisted string actuation system is required to pull the tendons around 35 mm. The force required is around 50 N for the flexion of the index and thumb finger, the remaining three fingers also require around 50 N of force to close. The closing time of the fingers must be less than 2 seconds.

The system requirements were introduced in the mathematical model and the required speed of the motors was determined. The torque requirements were experimentally found and the motors selected. The actuators that will be used are listed in Table 5.1.

Table 5.1 – Motors used in the robotic hand.

Motor	Stall Current at 6 V [A]	No-Load Speed at 6 V [r.p.m.]	Stall Torque at 6 V [N.m]	Movement associated with the actuator
30:1 Micro Metal Gearmotor HP	1.6	1000	0.06	Flexion of the thumb and index finger
30:1 Micro Metal Gearmotor HP	1.6	1000	0.06	Flexion of the three remaining fingers
298:1 Micro Metal Gearmotor HP	1.6	100	0.49	Thumb circumduction
Manufacturer: http://www.pololu.com/category/60/micro-metal-gearmotors				

Three switches will be used to find the systems zero references. When the system is initialized the actuators will be moved until the switches are activated and the origin of the system is found.

5.2. Assembly of the robotic hand

In this section, the assembly process of the robotic hand is demonstrated and the integration of the twisted string actuation system in the robotic hand is explained. Figure 5.5 shows the inside of the hand's palm, where the actuation system is assembled.

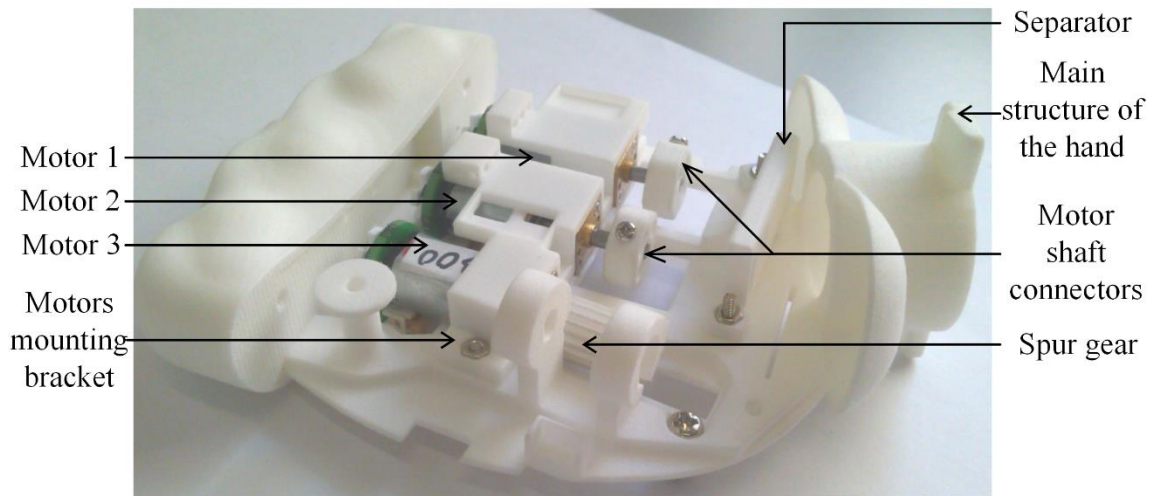


Figure 5.5 – Image of the internal components of the hand.

Figure 5.6 shows a photo of the hand with the palm cover. This cover has several purposes, such as protecting the internal components of the hand, reinforcing the structure of the hand, helping with the grasping of objects and providing a more anthropomorphic appearance.

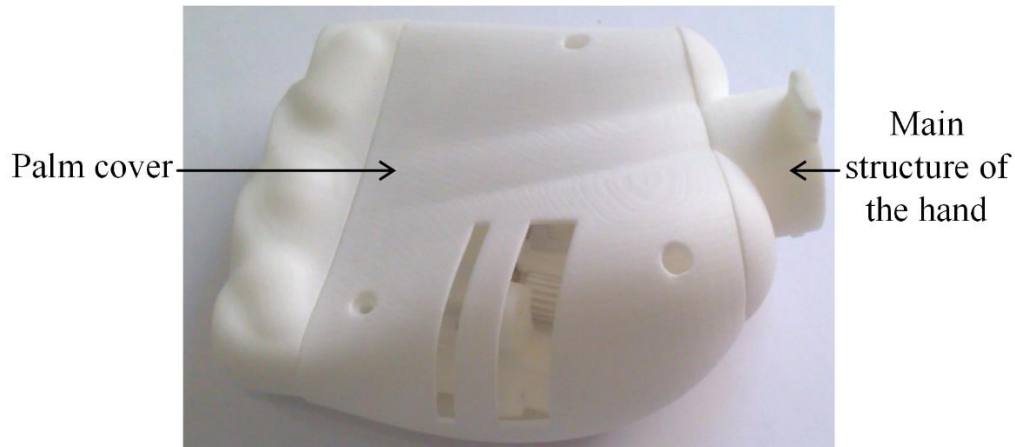


Figure 5.6 – Image of the hand with the palm cover placed.

In Figure 5.7 three of the fingers and the twisted string actuation system that controls them are placed in the hand. The fingers were built using a 3D printed internal structure which is later placed in a mold, where a urethane rubber will be poured. The building of the fingers was an important step of the assembly of the hand, however as was mentioned in the previous section, the fingers are not a part of this research, therefore the

building process will not be included here. For more information on the fingers building process, the reader is invited to see [14].

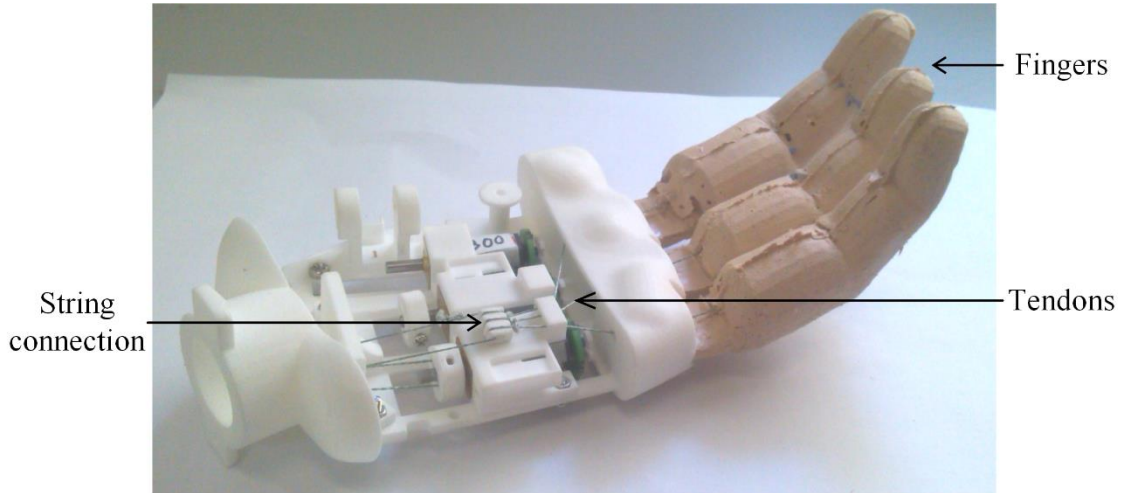


Figure 5.7 – Image of the hand with three of the fingers connected to the twisted string actuation system.

Figure 5.8 is a zoom of the twisted string actuation system and its integration in the hand. The tendons from the fingers are routed by the motors mounting bracket part. Then they are connected to the twisted strings using the string connection part. This part will also be used to touch the switch to indicate the zero reference. The twisted strings are connected to the motor shaft by a motor shaft connector part. The separator will be used to route the twisted strings, from the twisting zone to the linear displacement zone.

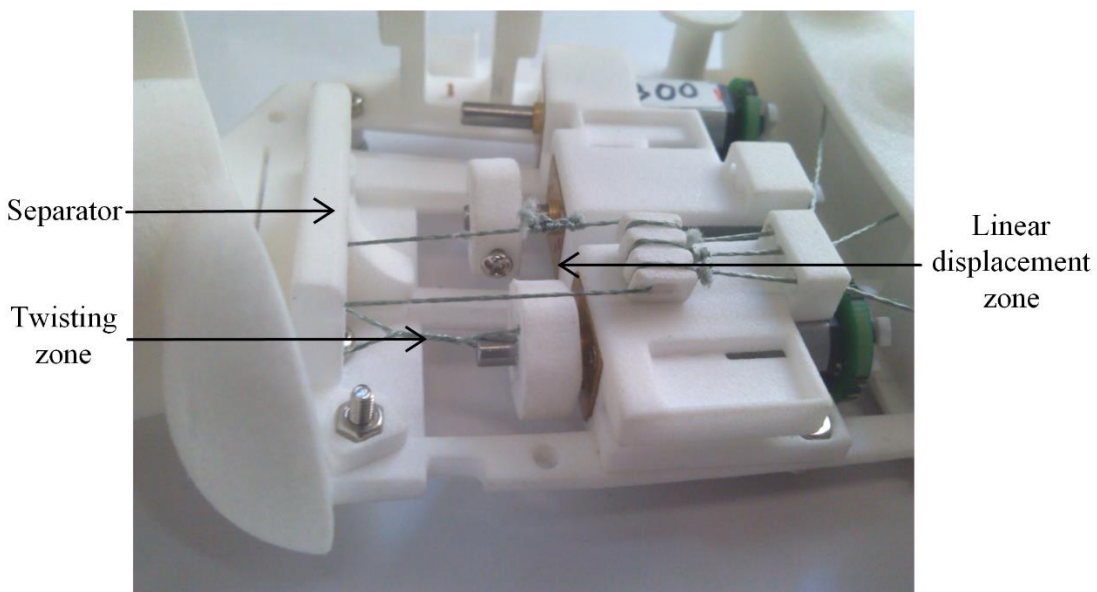


Figure 5.8 – Zoom of the twisted string system after a few turns of the motor shaft.

In contrast with the initial prototype, in which the twisting zone is placed in series with the linear displacement zone, here in order to save more space, we placed the twisting zone in parallel with the linear displacement zone. To do so, the separator has a tunnel that routes the tendons as can be seen in Figure 5.8.

The index and thumb fingers will be controlled with a similar twisted string actuation system coupled to motor 2. Figure 5.9 shows the photo of the complete hand.



Figure 5.9 – Photo of the robotic hand with all of the fingers placed.

The robotic hand has a length of around 210 mm, which is about the size of the average human hand. The human hand has an average weight of 400 grams, while the hand presented here weights around 240 grams, making it more than light enough to be used as a prosthetics device. When compared to existing prosthetics hands, such as the SmartHand [15], which has 4 actuators and weights 530 g, the light weight of the hand shown here becomes more evident. Figure 5.10 shows a comparison between the robotic hand with a human hand.



Figure 5.10 – Comparison of the robotic hand with a human one.

5.3. Control system for the robotic hand

To determine the position of the motors shafts, optical encoders were used. The three optical encoders are connected to a custom designed microcontroller printed circuit board, which is located inside of the hand (please check Figure 5.11). This circuit board is also connected to the three switches, the power supply and another custom designed microcontroller printed circuit board located on the outside of the hand.

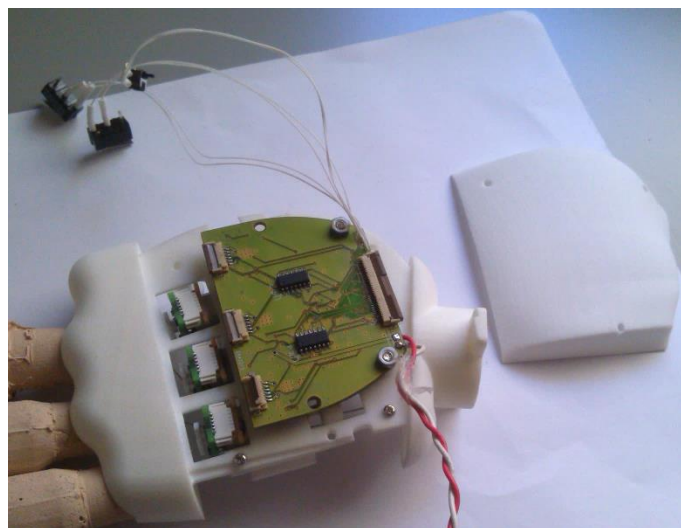


Figure 5.11 – Photo of the circuit board located inside of the hand.

The circuit board on the outside of the hand (please check Figure 5.12) communicates through a wireless connection with the computer.

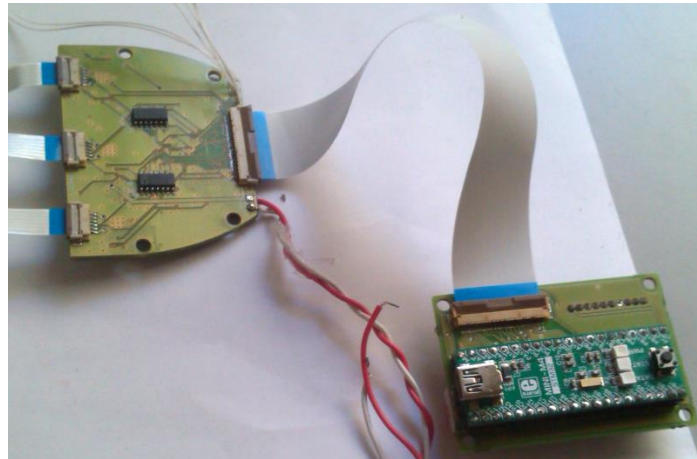


Figure 5.12 – Photo of both circuit boards used to control the hand.

Visual C# language was used to create an application to control the actuators in the hand (please check Figure 5.13).

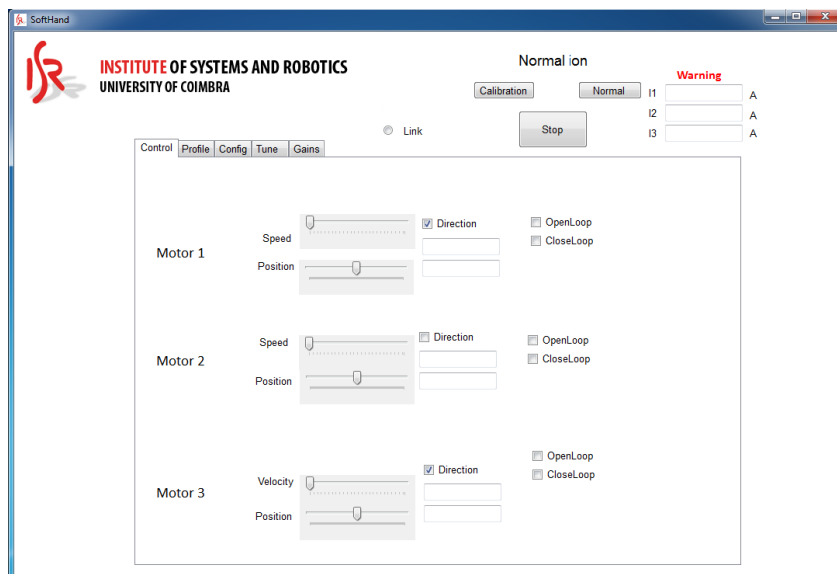


Figure 5.13 – Image of the GUI used to control the motors.

6. CONCLUSION

The twisted string actuation system is indeed a simple, low cost and effective linear actuator. Its major limitation, which is the low contraction ratio of existing systems, they have a maximum contraction ratio of around 25%, has been greatly improved by this research, which reached a maximum contraction ratio of 81% by using the two-phase twisted string actuation system. Such a high contraction ratio, leads to a more compact twisted string systems that can increase its range of applications. The first phase is the normal twist of two or more strings around each other. While the second phase is the overtwist phase, where the strings lack the space to twist normally and the entire string bundle twists around itself. Some authors reported that the overtwist phase can cause permanent damage to the strings. However, in our experiments the “Potenza Braided Line” from Vega, handled the overtwist phase without suffer any permanent damage. Therefore, the life cycle of the strings depends on the strings material and this should be subjected to further analysis. In conclusion, the overtwist phase allows for a high contraction ratio, probably at the cost of a reduced life of the strings.

We found out that existing mathematical models, for similar systems, cannot predict the linear displacement in the overtwist phase. Thus, an improved mathematical model is proposed in section 4, which can predict the linear displacement of the actuator for the entire range of contraction. The main contribution of this improved mathematical model is a better prediction of the string bundle radius.

The robotic hand presented in section 5, is an application of the compactness achieved due to this research. Another important achievement of the robotic hand, is its weight of 240 g, which is light compared to the human hand that has an average weight of 400g and compared to existing robotic hands. However, in a robotic hand with only three actuators, the major advantages of the twisted string actuation systems, such as low cost and light weight, are not so evident, because of the small number of actuators. If the number of actuators of the system is higher, like in the DEXMART hand, which has 24 actuators, then the advantages mentioned above will become more significant. Therefore there is a plan to build a new hand with a higher number of actuators, using several twisted string actuation

systems located in the forearm, similar to DEXMART hand, but in a more compact configuration.

Another future research plan are the development of the mathematical model to include an accurate torque prediction and its experimental verification. Moreover, the development of a twisted string actuation system with a constant transmission ratio that should allow for simpler control is also planned.

6.1. Publications

This research work as led to some novel solutions and because of that a manuscript entitled “A Compact Two-Phase Twisted String Actuation System: Modeling and Validation” has been submitted for possible publication in “Transactions on Mechatronics”.

7. REFERENCES

- [1] T. Sonoda, K. Ishii, A. A. F. Nassiraei and I. Godler, "Control of robotic joint by using antagonistic pair of Twist Drive Actuators," in *IECON 2012 - 38th Annual Conference on IEEE Industrial Electronics Society*, 2012.
- [2] G. Palli, S. Pirozzi, C. Natale, G. De Maria and C. Melchiorri, "Mechatronic design of innovative robot hands: Integration and control issues," in *Advanced Intelligent Mechatronics (AIM), 2013 IEEE/ASME International Conference on*, 2013.
- [3] I. Godler and T. Sonoda, "Performance evaluation of twisted strings driven robotic finger," in *Ubiquitous Robots and Ambient Intelligence (URAI), 2011 8th International Conference on*, 2011.
- [4] G. Palli, C. Natale, C. May, C. Melchiorri and T. Wurtz, "Modeling and Control of the Twisted String Actuation System," *Mechatronics, IEEE/ASME Transactions on*, vol. 18, no. 2, pp. 664-673, April 2013.
- [5] D. Popov, I. Gaponov and J.-H. Ryu, "A study on twisted string actuation systems: Mathematical model and its experimental evaluation," in *Intelligent Robots and Systems (IROS), 2012 IEEE/RSJ International Conference on*, 2012.
- [6] D. Popov, I. Gaponov and J. Ryu, "A preliminary study on a twisted strings-based elbow exoskeleton," in *World Haptics Conference (WHC), 2013*, 2013.
- [7] "Climbing and Walking Robots, Towards New Applications," Itech Education and Publishing, 2007.
- [8] M. Suzuki and A. Ichikawa, "Toward Springy Robot Walk Using Strand-Muscle Actuators," in *Proc. 7th Int. Conf. Climbing and Walking Robots*, Madrid, 2004.
- [9] M. Suzuki, T. Mayahara and A. Ishizaka, "Redundant muscle coordination of a multi-DOF robot joint by online optimization," in *Advanced intelligent mechatronics, 2007 IEEE/ASME international conference on*, 2007.
- [10] I. Godler and T. Sonoda, "A Five Fingered Robotic Hand Prototype by using Twist Drive," in *Robotics (ISR), 2010 41st International Symposium on and 2010 6th German Conference on Robotics (ROBOTIK)*, 2010.

- [11] D. Popov, I. Gaponov and J.-H. Ryu, "Bidirectional elbow exoskeleton based on twisted-string actuators," in *Intelligent Robots and Systems (IROS), 2013 IEEE/RSJ International Conference on*, 2013.
- [12] Y. J. Shin, H. J. Lee, K.-S. Kim and S. Kim, "A Robot Finger Design Using a Dual-Mode Twisting Mechanism to Achieve High-Speed Motion and Large Grasping Force," *Robotics, IEEE Transactions on*, vol. 28, no. 6, pp. 1398-1405, Dec 2012.
- [13] I. Gaponov, D. Popov and J.-H. Ryu, "Twisted String Actuation Systems: A Study of the Mathematical Model and a Comparison of Twisted Strings," *Mechatronics, IEEE/ASME Transactions on*, vol. 19, no. 4, pp. 1331-1342, Aug 2014.
- [14] M. Tavakoli and A. T. de Almeida, "Adaptive under-actuated anthropomorphic hand: Isr-softhand," in *2014 IEEE/RSJ International Conference on Intelligent Robots and Systems (IROS)*, Chicago, 2014.
- [15] C. Cipriani, M. Controzzi and M. C. Carrozza, "The SmartHand transradial prosthesis," *Journal of NeuroEngineering and Rehabilitation*, vol. 8, p. 29, 2011.